Soils and Rocks
An International Journal of Geotechnical and Geoenvironmental Engineering
www.soilsandrocks.com
ISSN 1980-9743
ISSN-e 2675-5475

Numerical investigation of reverse fault rupture impact on single pile and shallow foundation performance

Ali Safari[1], Ali Nabizadeh[1#]

Article

Keywords
Reverse fault rupture
Fault–foundation interaction
Finite element modeling
Single pile
Shallow foundation

Abstract

Fault-induced permanent ground deformation poses a serious threat to foundations located near active reverse faults. This study numerically investigates the coupled response of a shallow foundation and a single pile subjected to reverse fault rupture using a two-dimensional finite element model. The numerical framework is developed based on centrifuge test configurations and validated against experimental observations in terms of rupture trajectory, foundation deformation, and pile response. The results demonstrate a strong coupled interaction between the shallow foundation and the pile. The presence of the pile significantly increases the rotation and lateral displacement of the shallow foundation, while the shallow foundation alters the surrounding soil stress field and leads to higher bending moments along the pile. Parametric analyses conducted for different normalized fault offsets (h/H) demonstrate that increasing fault displacement intensifies stress concentration and expands the plastic zone in the vicinity of the pile–foundation system. The findings emphasize that shallow and deep foundation elements should not be designed independently in fault-affected regions, and that coupled soil–foundation interaction should be considered to improve seismic resilience under reverse fault rupture.

1. Introduction

Ground deformations induced by surface-fault rupture represent one of the most critical hazards for infrastructure located near active fault zones. In reverse faulting, the imposed permanent ground deformation (PGD) may lead to severe differential settlement, rotation, and stress concentration in foundation systems, potentially compromising both serviceability and stability. Therefore, understanding the mechanisms of fault–foundation interaction is essential for improving seismic resilience and supporting rational foundation design in fault-affected regions.

Extensive experimental and numerical studies have investigated the response of shallow foundations subjected to reverse fault rupture. Centrifuge model tests have shown that foundation stiffness, embedment depth, and bearing pressure strongly influence rupture diversion and foundation rotation (e.g., Bransby et al., 2008; Ahmed & Bransby, 2009; Ashtiani et al., 2016; Guan et al., 2025). In parallel, numerical investigations have provided valuable insight into stress redistribution and deformation mechanisms and have enabled parametric studies on fault geometry and foundation configuration (e.g., Anastasopoulos et al., 2010; Baziar et al., 2015; Liu et al., 2021). However, most studies have primarily focused on shallow foundations alone.

On the other hand, the response of piles subjected to dip-slip faulting has also been examined through physical and numerical modeling (e.g., Anastasopoulos et al., 2013). Recent centrifuge experiments have clarified the development of pile bending moments and lateral displacements with increasing fault offset (Yao & Takemura, 2020), and simplified analytical models have also been proposed for single piles under reverse faulting (Guo et al., 2025). Nevertheless, these investigations typically considered isolated piles, without accounting for the influence of an overlying shallow foundation and the resulting coupled interaction between shallow and deep foundation elements.

In practice, shallow and deep foundation systems often coexist and interact, and their interaction may significantly alter both the rupture propagation pattern and the structural response. The presence of a pile can modify the deformation field and constrain soil movement, while the shallow foundation can redistribute stresses and affect pile bending demands. Despite the relevance of this coupled mechanism, the mutual interaction between a shallow foundation and a single pile subjected to reverse fault rupture remains insufficiently quantified, particularly in terms of stress transfer, plastic zone development, and foundation rotation.

Accordingly, this study presents a validated two-dimensional finite element investigation of a coupled shallow

#Corresponding author. E-mail address: ali.nabizadeh@sru.ac.ir
[1]Shahid Rajaee Teacher Training University, Department of Civil Engineering, Tehran, Iran.

Submitted on December 14, 2025; Final Acceptance on August 15, 2026; Discussion open until May 31, 2027.
Editor: Renato P. Cunha
https://doi.org/10.28927/SR.2027.020125

This is an Open Access article distributed under the terms of the Creative Commons Attribution license (https://creativecommons.org/licenses/by/4.0/), which permits unrestricted use, distribution, and reproduction in any medium, provided the original work is properly cited.

foundation–single pile system subjected to reverse fault rupture. The numerical model is developed based on centrifuge test configurations reported by Yao et al. (2021) and is validated against experimental observations in terms of rupture trajectory, pile deformation, and foundation response. The validated framework is then employed to examine the mutual interaction between the shallow foundation and the pile, with emphasis on (i) rupture propagation and stress redistribution, (ii) development of plastic zones and failure mechanisms, and (iii) changes in foundation rotation and pile bending moments under different normalized fault offsets. The findings provide insight into the conditions under which pile–foundation interaction may amplify or modify structural demands and highlight the importance of considering coupled foundation systems in seismic design near active reverse faults.

The novelty of this study lies in quantifying the coupled response of a shallow foundation and a single pile under reverse fault rupture within a validated numerical framework. Unlike most previous studies that investigated shallow foundations or piles separately, this work focuses on the interaction mechanisms between the two foundation components, including stress redistribution, foundation rotation amplification, pile bending demand, and plastic strain localization. The results provide mechanistic insight into how the presence of one foundation element modifies the response of the other, which is directly relevant for assessing foundation performance in fault-affected ground.

Such configurations may occur in retrofitting scenarios, bridge abutments supported by piles beneath shallow footings, or in foundation systems combining shallow load distribution with deep anchorage for seismic resilience.

2. Materials and methods

To ensure the reliability of the numerical simulations, the finite element (FE) model developed in this study was validated against centrifuge test results reported by Yao et al. (2021). Two test configurations, namely RPL and RPH, were selected. These tests investigated the interaction between a shallow foundation and a single pile subjected to reverse fault rupture in dry Toyoura sand under a centrifugal acceleration of 50 g. The centrifuge measurements provide key reference data, including rupture propagation patterns, foundation displacement and rotation, pile lateral deformation, bending moment profiles, and soil deformation fields. These experimental observations were used to calibrate and validate the numerical framework.

The numerical model was established to reproduce the centrifuge test geometry at prototype scale. A two-dimensional plane strain FE model was adopted, with a soil domain 25 m wide and 11 m deep and a reverse fault plane inclined at 60° to the horizontal (Figure 1). The single pile had a diameter of 0.5 m and an embedded length of 10.5 m. A 2.5 m-wide shallow foundation was placed concentrically above the pile. The shallow foundation was modeled as a rigid cap in direct contact with the pile head, consistent with the centrifuge configuration, allowing load transfer and rotation compatibility between the two components. The bottom boundary of the model was restrained in both horizontal and vertical directions, while the lateral boundaries were assigned roller constraints allowing vertical displacement and restricting horizontal movement. The adopted domain size and boundary conditions were selected to minimize boundary effects on stress redistribution and rupture propagation in the region of interest.

Although fault–foundation interaction is inherently three-dimensional, a two-dimensional plane strain approach was employed in this study for two main reasons. First, the numerical framework was directly developed to replicate and validate against the available centrifuge test configurations, which were interpreted and reported mainly in terms of cross-sectional deformation mechanisms.

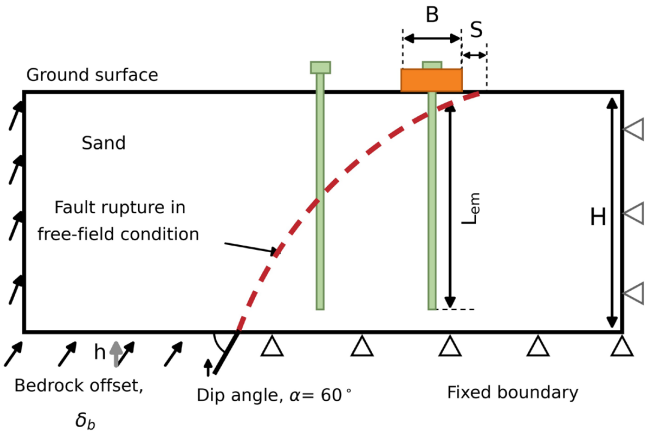


Figure 1. Geometry of the 2D numerical model showing the reverse fault, single pile, and shallow foundation with boundary conditions (Yao et al., 2021).

Second, the main objective of this study is to investigate the fundamental interaction mechanisms between a shallow foundation and a single pile during reverse fault rupture, including rupture diversion, stress redistribution, plastic zone development, and foundation rotation, which can be effectively captured in a representative plane strain section. Nevertheless, it should be acknowledged that out-of-plane effects such as three-dimensional pile bending, torsional response, and spatial variability of rupture diversion cannot be fully reproduced. Therefore, the results should be interpreted as representative cross-sectional interaction mechanisms rather than a complete 3D description of the foundation system.

Reverse faulting was simulated through a two-step loading procedure. In the first step, gravity loading was applied to establish the initial geostatic stress state. In the second step, reverse fault rupture was simulated by imposing a prescribed vertical displacement at the base of the model across the predefined 60° fault plane. The displacement was applied incrementally under quasi-static conditions, and the cumulative vertical bedrock offset was 2.6 m, consistent with the prototype-scale displacement used in the centrifuge tests. A dynamic implicit procedure with sufficiently slow loading rate and adequate time scaling was employed to ensure quasi-static conditions while enabling stable simulation of large deformation and strain localization associated with rupture propagation. Inertial effects were minimized by applying the displacement gradually and ensuring that kinetic energy remained negligible compared to internal energy during the analysis.

The soil was modeled using the Mohr–Coulomb elastoplastic constitutive model, which is widely adopted for simulating the behavior of dry sands in fault–foundation interaction problems. The model parameters, including unit weight, Young's modulus, Poisson's ratio, internal friction angle, and dilation angle, were selected based on the centrifuge test conditions reported by Yao et al. (2021). The yield criterion is defined by the friction angle (φ) and cohesion (c), while plastic flow is governed by a non-associated flow rule controlled by the dilation angle (ψ). Since Toyoura sand is a clean dry sand, cohesion was taken as negligible. The model assumes elastic behavior up to yield and perfectly plastic response after yielding, without strain hardening or softening. This simplified framework was selected to maintain consistency with the centrifuge calibration data and to focus on the rupture-induced kinematic interaction mechanisms. The acrylic pile and brass shallow foundation were modeled as linear elastic materials. The adopted material properties are summarized in Table 1.

Figure 1 illustrates the general geometry of the two-dimensional model and the relative position of the shallow foundation and pile with respect to the fault zone, as well as the applied boundary conditions. The numerical configuration was established to be consistent with the centrifuge test setup, enabling direct comparison of key outputs such as rupture trajectory, foundation deformation, pile displacement, and bending moment distribution along the pile.

To investigate the influence of fault displacement magnitude on the coupled pile–foundation response, three normalized fault offsets were considered in terms of the ratio h/H, where h is the applied vertical bedrock offset and H = 11 m is the soil layer thickness. The analyzed cases correspond to h/H values of 2.36%, 7.09%, and 11.81%. These cases enabled systematic evaluation of progressive deformation, foundation rotation, pile displacement, stress redistribution, and plastic zone development with increasing fault offset.

The soil domain was discretized using four-node plane strain elements with reduced integration (CPE4R). A structured mesh was adopted, with refinement in the vicinity of the pile and shallow foundation where high strain gradients and rupture localization occur. The nominal element size in the refined zone was 0.6 m × 0.6 m. A mesh sensitivity analysis was conducted to confirm that the predicted rupture trajectory, foundation rotation, and pile response were not significantly influenced by mesh density, ensuring that the reported results are not affected by numerical artifacts associated with strain localization. Mesh sensitivity was evaluated by repeating selected analyses using finer and coarser discretizations in the rupture and foundation vicinity. The maximum variation in computed foundation rotation and pile head displacement between the refined and coarser meshes was less than 3%, indicating that the adopted mesh is sufficiently objective and not significantly influenced by mesh-dependent strain localization. The selected mesh was therefore considered adequate to capture the main deformation mechanisms while avoiding excessive computational cost.

Soil–structure interaction was modeled using surface-to-surface contact with a frictional formulation and penalty enforcement. This approach was adopted to represent interface shear transfer between the soil and the pile/foundation surfaces. Different interface friction coefficients were assigned to the pile–soil and foundation–soil contacts to reflect material-specific interface behavior. A friction coefficient of μ = 0.30 was adopted for the pile–soil interface, while μ = 0.394 was used for the foundation–soil interface.

Table 1. Properties of the materials adopted in the numerical modeling.

Material	Unit weight (kN/m^3)	Elastic modulus (GPa)	Poisson's ratio	Friction angle (degree)
Toyoura Sand	15.8	0.013	0.30	48.5
Single Pile (Acrylic)	11.8	0.00504	0.35	–
Foundation (Brass)	85	110	0.33	–

CC BY

These values were selected based on reported interface properties for Toyoura sand in contact with acrylic (pile material) and brass (foundation material) under dry conditions, consistent with the centrifuge test configuration. The FE simulations were carried out using a dynamic implicit procedure with a sufficiently slow loading rate and adequate time scaling to maintain quasi-static conditions while enabling stable numerical computation of large deformation and rupture propagation. Inertial effects were controlled by applying the imposed fault displacement gradually and verifying that kinetic energy remained negligible compared to internal energy throughout the analysis.

It should be noted that the investigated problem is inherently three-dimensional, particularly regarding pile bending and out-of-plane stress redistribution. In this study, a two-dimensional plane strain model was adopted as a computationally efficient approach, consistent with the numerical framework used in several previous fault–foundation interaction studies. While the adopted model captures the dominant kinematic effects of reverse fault rupture and provides good agreement with centrifuge observations, three-dimensional effects such as non-uniform pile curvature and torsional response are not represented. Therefore, the results should be interpreted as representative trends and comparative mechanisms rather than exact field-scale predictions.

3. Analysis and results

3.1 Comparison between numerical and centrifuge tests

To validate the developed numerical model, key outputs were compared with centrifuge test results reported by Yao et al. (2021). The RPL and RPH configurations were selected because they provide experimental evidence for rupture propagation, foundation deformation, and pile response. The validation is performed through comparison of (i) fault rupture trajectory, and (ii) pile response indicators such as lateral displacement and bending moment profiles. The following subsections present the main agreements between numerical predictions and experimental observations, and briefly discuss the sources of minor discrepancies.

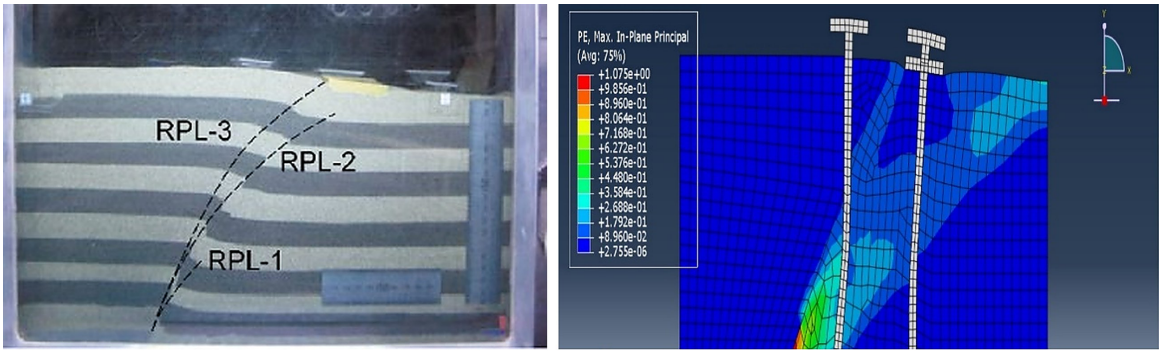
3.1.1 Fault rupture path

One of the most important aspects of reverse faulting is the rupture trajectory developing through the soil mass, including its direction, curvature, and surface emergence location. Accurate prediction of rupture propagation is essential for assessing the potential impact on nearby foundation elements. In this section, the rupture path obtained from the numerical model is compared with centrifuge observations for Cases RPL and RPH to evaluate the model's capability in reproducing reverse fault rupture mechanisms.

The rupture trace observed in the centrifuge experiment is shown in Figure 2. The rupture initiates at the base of the inclined fault plane and propagates upward toward the ground surface. In the physical model (Figure 2a), the rupture emerges slightly to the left of the pile and follows a curved trajectory. Similarly, in the numerical simulation (Figure 2b), the zone of maximum principal strain indicates a comparable rupture path and surface emergence location.

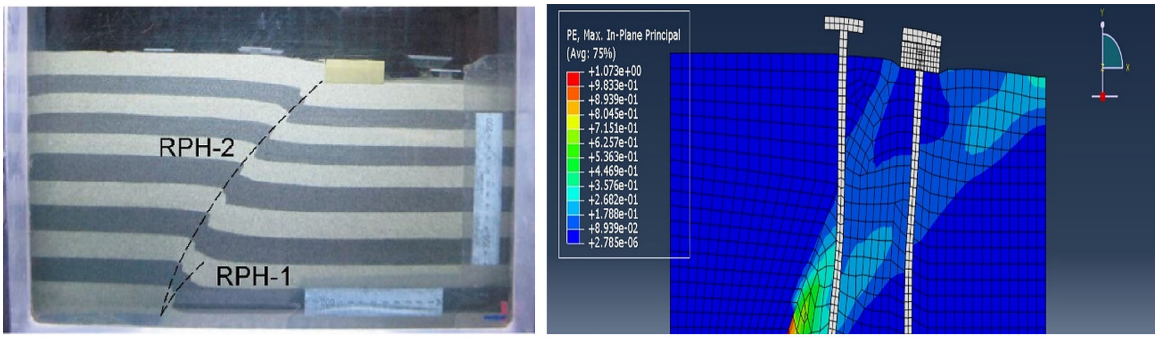
The presence of the pile influences rupture propagation in both the experiment and the numerical model. In the centrifuge test, the rupture trajectory is partially diverted as it approaches and interacts with the pile shaft. In the numerical simulation, strain localization intensifies around the pile before the rupture propagates toward the ground surface. Overall, the comparison demonstrates that the numerical model captures the key features of rupture–structure interaction and reproduces the main rupture propagation pattern observed in the centrifuge tests.

In addition to Case RPL, Case RPH was analyzed to further evaluate the performance of the numerical model under reverse faulting. This configuration features a different pile location relative to the rupture zone, allowing the influence of pile position on rupture propagation to be assessed.



(a) **(b)**

Figure 2. Comparison of fault rupture paths in Case RPL: (a) rupture trace observed in the centrifuge test, and (b) principal strain contours from the numerical simulation showing the rupture zone.



(a) **(b)**

Figure 3. Comparison of fault rupture paths in Case RPH: (a) rupture trace observed in the centrifuge test, and (b) principal strain contours from the numerical simulation showing the rupture zone.

The rupture trace observed in the centrifuge test is compared with the numerical principal strain contours in Figure 3.

The failure pattern of Case RPH shows good agreement between the centrifuge observations and the numerical results. As shown in Figure 3, the rupture initiates at the base of the inclined fault plane and propagates upward through the soil mass before emerging at the ground surface along a curved trajectory. In the physical model (Figure 3a), the rupture bypasses the pile and reaches the surface at a location to the right of the pile shaft. A similar response is captured in the numerical simulation (Figure 3b), where the zone of maximum principal strain follows essentially the same path and surface emergence point.

Compared with Case RPL, the pile in this configuration is located farther from the primary rupture zone, resulting in reduced interaction between the pile and the propagating fault. Consequently, the rupture trajectory appears smoother and less deflected in both the experiment and the numerical model. These results further confirm the ability of the developed numerical framework to reproduce different rupture propagation patterns as a function of pile position, thereby supporting the robustness of the adopted modeling approach.

3.1.2 Pile horizontal displacement

Pile head and shaft displacements are key indicators of pile performance under fault-induced ground deformation. In this section, the lateral displacement profiles obtained from the numerical model are compared with centrifuge measurements for Cases RPL and RPH. The comparison is performed along the pile depth to evaluate the ability of the model to reproduce both the displacement trend and its magnitude.

The horizontal displacement profile of the pile in Case RPL, which is located within the main rupture zone, is presented in Figure 4. Overall, the numerical results show good agreement with the centrifuge measurements,

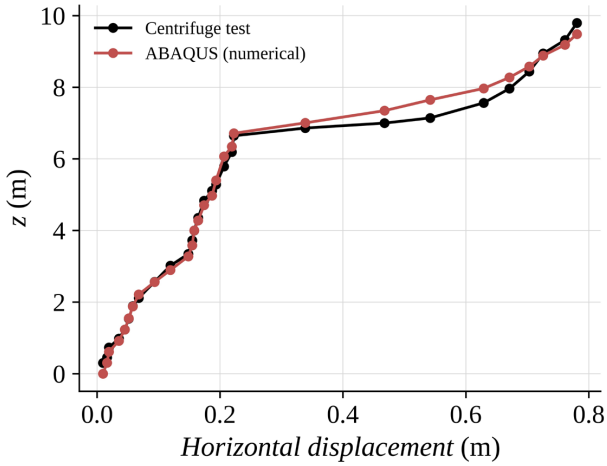


Figure 4. Comparison of horizontal displacement profiles of the single pile along depth for Case RPL: centrifuge test versus numerical simulation.

particularly in the upper portion of the pile. Both datasets indicate a consistent deformation trend, with the maximum lateral displacement occurring near the ground surface due to fault-induced shearing and progressive rupture propagation.

The numerical model captures the pile deformation pattern reasonably well, especially within the upper 0–6 m depth where fault-induced soil movement is most pronounced. Minor differences at greater depths may be attributed to local variations in soil–pile interface response and experimental measurement uncertainty. In general, the comparison confirms that the adopted numerical framework can reproduce the main characteristics of pile lateral displacement when the pile is located within the rupture-affected zone.

To further evaluate the influence of pile position relative to the fault, the displacement profiles for both RPL and RPH configurations are presented together in Figure 5, enabling direct comparison of pile response as a function of proximity to the rupture zone.

Figure 5 compares the horizontal displacement profiles of the single pile in Cases RPL and RPH. In these two configurations, the pile is located at the same position relative to the fault, while the shallow foundation size is different. The results show that in Case RPH, where a larger shallow foundation is used, the pile experiences noticeably greater lateral displacements along most of its embedded length compared to Case RPL.

This behavior suggests that the larger foundation, due to its higher stiffness and wider contact area, induces stronger soil–foundation interaction during fault-induced ground deformation. As a result, larger horizontal demands are transferred from the foundation–soil system to the adjacent pile. In contrast, the smaller foundation in Case RPL leads to a comparatively lower displacement profile, particularly at mid-depth of the pile.

Quantitatively, the difference between numerical and centrifuge measurements in terms of maximum pile head displacement was within approximately 5–8%, and the overall displacement trend along the pile depth was well reproduced.

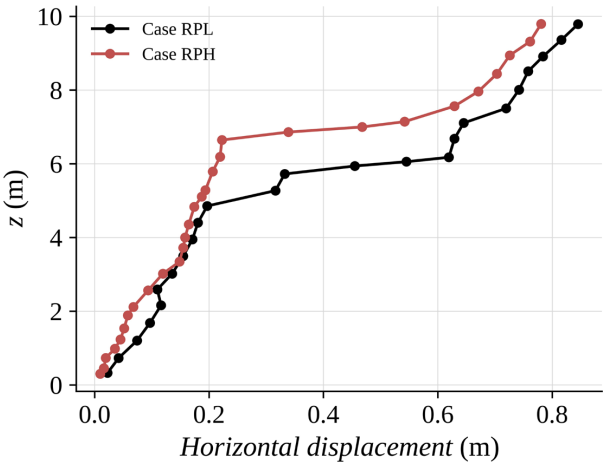


Figure 5. Comparison of horizontal displacement profiles of the single pile along depth in Cases RPL and RPH.

This level of agreement supports the reliability of the adopted numerical framework for investigating rupture–foundation interaction mechanisms.

Overall, the comparison highlights the significant influence of shallow foundation size on the pile deformation response under reverse fault rupture and confirms the sensitivity of the developed numerical model to variations in foundation geometry.

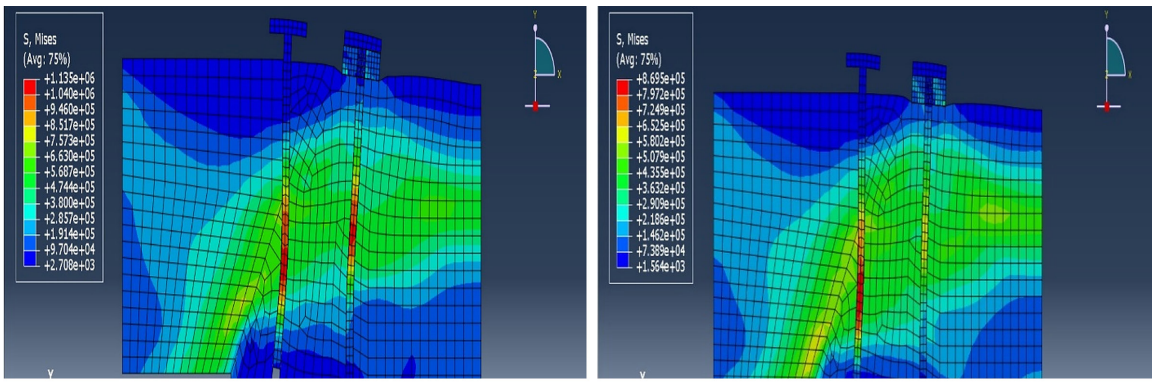
3.2 Numerical insights from the finite element model

3.2.1 Stress distribution in soil

One key advantage of the numerical approach is that it enables examination of internal stress redistribution within the soil mass, which cannot be directly measured in centrifuge tests. In the following subsection, stress contours are presented for different fault offset cases to further investigate the interaction between reverse fault rupture and the pile–foundation system. Both shear and vertical stress fields are examined to identify stress concentration zones and to assess the extent of stress transfer from the structural elements into the surrounding ground.

A comparison of Figures 6a and 6b illustrates the influence of fault offset magnitude on the soil stress response. At the higher offset level (Figure 6a, $h/H = 11.81\%$), a wider zone of elevated stress develops around the pile–foundation system, and the stress concentration extends deeper into the soil mass. This indicates stronger mobilization of soil resistance and more pronounced soil–structure interaction under larger fault-induced deformation.

In contrast, at the lower offset level (Figure 6b, $h/H = 7.09\%$), the stress concentration zone remains more localized and less extensive, reflecting a reduced level of soil mobilization and interaction demand. Overall, the results confirm that increasing fault displacement leads to stronger stress redistribution and a broader affected zone in the surrounding ground.



(a) **(b)**

Figure 6. Distribution of von Mises stress in the soil domain at two levels of fault ratio: (a) h/H = 11.81%, and (b) h/H = 7.09%.

To evaluate the effect of foundation geometry on stress redistribution, two numerical cases (RPL and RPH) with identical pile and faulting conditions but different shallow foundation dimensions were compared. The resulting stress contours provide insight into how the foundation size influences stress concentration beneath the footing and around the pile during reverse faulting.

Figure 7 presents the stress distribution for two shallow foundation geometries with the same lengths (2.5 m) but different thickness. In Case RPH (Figure 7a), where the foundation thickness is 1.0 m, the stress field beneath the foundation is more distributed, with a wider affected zone in the surrounding soil. In contrast, in Case RPL (Figure 7b), where the foundation thickness is 0.5 m, higher stress concentrations develop beneath the footing and in the vicinity of the pile.

The comparison suggests that the thinner foundation promotes more localized stress transfer into the soil, which intensifies the interaction between the shallow foundation and the adjacent pile. These results highlight the importance of shallow foundation dimensions—particularly foundation thickness—in controlling stress redistribution patterns under reverse fault rupture.

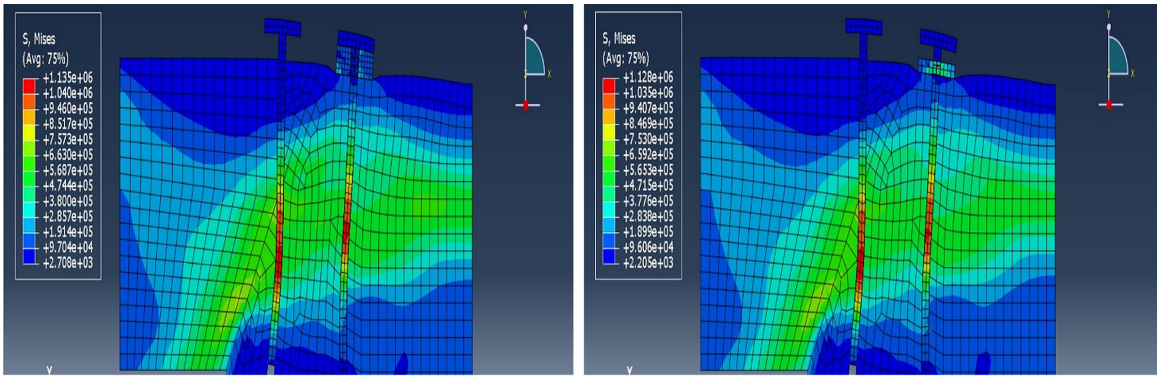
3.2.2 Foundation rotation

Foundation rotation is a key indicator of performance and stability under reverse fault–induced ground deformation, as it directly reflects asymmetric soil–foundation interaction and differential movement beneath the footing. Compared to settlement or lateral translation, rotation provides a clearer measure of the non-uniform contact pressure distribution that develops during rupture propagation. Although the centrifuge tests by Yao et al. (2021) did not explicitly report foundation rotation, the numerical model enables direct evaluation of this response.

To investigate the influence of foundation geometry and pile interaction on rotation, Cases RPL and RPH are compared. These two cases share identical soil properties, faulting conditions, and pile location, while the shallow foundation geometry is varied to isolate its effect. In addition, Case RH (without pile) is included to quantify the role of the pile in modifying rotational response.

Table 2 summarizes the computed foundation rotations for the analyzed configurations. The results indicate that the rotation in the piled cases (RPL and RPH) is significantly larger than in the unpiled case (RH). While RH exhibits a very small rotation of 0.015°, the rotation increases to approximately 0.26° when a pile is present. This increase highlights the strong influence of the pile on constraining soil deformation and altering the stress transfer mechanism beneath the footing.

A comparison between RPL and RPH shows that changing the foundation thickness from 0.5 m to 1.0 m (in the investigated parameter) results in only a marginal change in rotation (0.257° to 0.261°), corresponding to a difference of less than 2%. This suggests that, under the considered fault offset and soil conditions, the pile–soil interaction dominates the rotational response, whereas the investigated foundation thickness variation plays a secondary role.



(a) **(b)**

Figure 7. Von Mises stress distribution in two shallow foundation configurations with identical length (2.5 m) and different thickness: (a) 1.0 m (RPH), and (b) 0.5 m (RPL).

Table 2. Comparison of foundation rotation under reverse faulting for three foundation configurations.

Case	Foundation Thickness (m)	Pile Present	Rotation (deg)
RH	1.0	No	0.015°
RPL	0.5	Yes	0.257°
RPH	1.0	Yes	0.261°

CC BY

Mechanically, the pile acts as a stiff inclusion that restrains free kinematic deformation of the soil mass during fault-induced shearing. This restraint leads to asymmetric stress redistribution around the pile and the foundation base, generating an additional overturning moment and increasing foundation rotation. The results therefore indicate that, for shallow foundations located near reverse faults, the presence of a pile can significantly modify the rotation demand and should be explicitly considered in coupled soil–structure interaction assessments.

3.2.3 Plastic zones and failure mechanism

Understanding the development of plastic zones is essential for interpreting the failure mechanisms governing soil–foundation interaction under reverse faulting. While centrifuge tests provide valuable observations of overall deformation patterns, they are limited in revealing internal yielding and plastic strain localization within the soil mass. In contrast, finite element modeling enables direct assessment of stress redistribution, progressive yielding, and the evolution of localized plastic zones, particularly around critical interfaces such as the pile shaft and foundation base.

In this section, the spatial distribution and growth of plastic strain zones are examined to identify key mobilized regions and to clarify the mechanisms through which reverse fault displacement leads to localized yielding and potential failure surfaces. Special attention is given to the influence of the pile on modifying plasticity patterns and promoting strain localization near the soil–structure interfaces.

As shown in Figure 8, comparison of equivalent plastic strain (PEEQ) contours for Cases RPL and RPH indicates clear differences in the extent and geometry of plastic zone development under reverse faulting. In Case RPL, with the thinner foundation (0.5 m), plastic strain remains relatively localized and vertically limited. The plastic zone initiates at the fault tip and develops beneath the shallow foundation and in the vicinity of the adjacent pile, suggesting a more concentrated deformation mechanism.

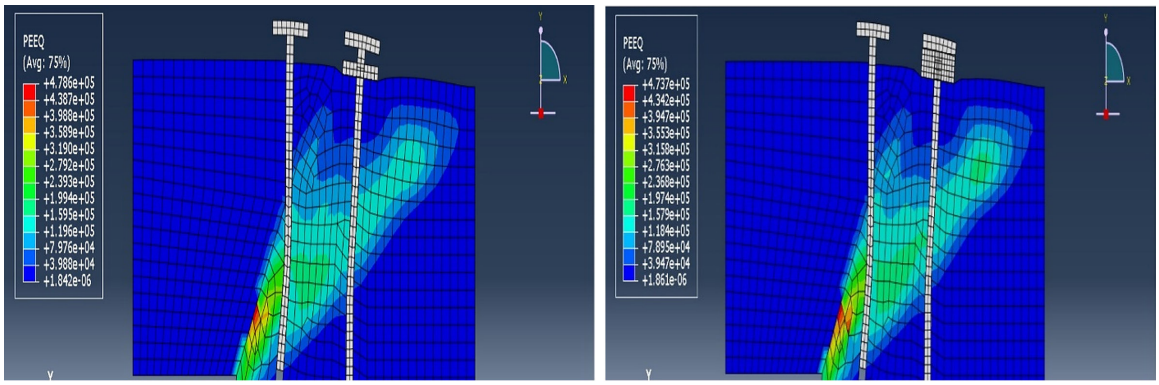
In contrast, Case RPH, with the thicker foundation (1.0 m), exhibits a wider and more laterally distributed plastic zone. The stiffer foundation tends to redistribute the fault-induced stresses over a larger area, resulting in a broader plastic deformation pattern. In this configuration, plastic strains extend deeper into the soil mass and propagate farther laterally, indicating a transition from localized yielding to a more distributed mobilization of the surrounding ground.

Overall, the results suggest that foundation thickness influences the failure mechanism by modifying stress transfer and deformation localization beneath the footing. Although pile–soil interaction occurs in both cases, the thicker foundation in RPH promotes a more gradual redistribution of stresses into the surrounding soil, which affects both the shape and extent of the developed plastic zones.

To further quantify the influence of the pile on the failure mechanism, a comparison between Cases RPH and RH is conducted. Since both configurations have the same foundation thickness (1.0 m), this comparison allows direct assessment of how the pile modifies stress redistribution and plastic strain localization under identical faulting conditions.

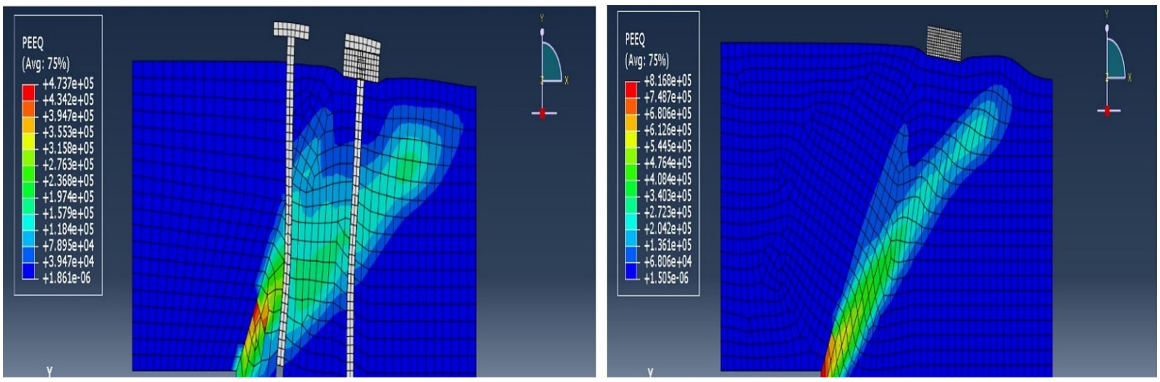
Figure 9 compares the equivalent plastic strain (PEEQ) contours for Cases RPH (with pile) and RH (without pile). In Case RH (Figure 9b), the plastic zone initiates at the fault tip and propagates upward along a relatively narrow trajectory toward the ground surface. The absence of a pile allows the soil to deform more freely, resulting in a comparatively smoother and more continuous failure mechanism with limited disturbance beneath the shallow foundation.

In contrast, Case RPH (Figure 9a) shows that the presence of the pile significantly alters the plastic deformation mechanism. The pile acts as a stiff inclusion that restrains kinematic soil movement, leading to stress concentration and localized plastic strain development around the pile–soil interface. As a result, the plastic zone becomes wider and more laterally distributed, with intensified yielding near the pile shaft and beneath the foundation.



(a) **(b)**

Figure 8. PEEQ contours for RPL (a) and RPH (b) showing plastic strain distribution under reverse faulting.



(a) **(b)**

Figure 9. PEEQ contours for RPH (a) and RH (b) showing plastic strain distribution under reverse faulting.

Overall, the comparison indicates that while reverse fault rupture in the unpiled configuration (RH) produces a relatively uniform plastic deformation pattern, the addition of a pile (RPH) introduces complex soil–structure interaction effects that modify both the intensity and geometry of plastic strain localization. This highlights the importance of considering coupled pile–foundation response when evaluating failure mechanisms in fault-affected ground.

From an engineering perspective, the results suggest that adding a pile beneath a shallow foundation in fault-affected ground does not necessarily reduce rotation demand. Instead, the pile may increase foundation rotation by constraining soil deformation and generating additional overturning moments. Therefore, simplified design approaches that treat shallow foundations and piles independently may underestimate rotation and bending demands when rupture occurs in close proximity.

4. Conclusions

This study presented a numerical investigation of reverse fault rupture effects on the response of a single pile, a shallow foundation, and their coupled interaction using finite element simulations. The numerical model was validated against centrifuge test results reported by Yao et al. (2021), demonstrating its ability to reproduce key mechanisms including rupture propagation, soil deformation patterns, and pile–foundation interaction.

The main findings can be summarized as follows:

- The presence of a single pile influences reverse fault rupture propagation by inducing stress concentration and local deviation of the rupture trajectory. The numerical simulations reproduced the experimentally observed rupture patterns with good agreement;
- Significant interaction was observed between the shallow foundation and the pile. The pile increased foundation rotation and lateral displacement, while the shallow foundation modified the near-field stress redistribution and contributed to increased bending demand along the pile shaft;
- Parametric comparisons indicated that the investigated foundation geometry variation affects plastic zone development and stress redistribution. The stiffer foundation configuration promoted a wider and more distributed plastic strain field, whereas the thinner foundation configuration led to more localized plastic deformation concentrated beneath the footing and near the pile;
- Comparing piled and unpiled cases showed that the pile alters the failure mechanism by restricting free soil deformation and promoting asymmetric plastic strain localization around the pile–soil interface. In contrast, the shallow foundation without a pile exhibited a more continuous and vertically propagating plastic deformation mechanism.

Overall, the results indicate that shallow foundations and piles located in reverse fault–affected ground may exhibit strong coupled behavior and should be assessed using an integrated soil–foundation interaction approach in similar scenarios. The findings contribute to a better understanding of fault–foundation interaction mechanisms and may support more resilient foundation design near active reverse faults.

The present study has some limitations that should be considered when interpreting the results. The numerical investigation was based on a two-dimensional plane strain model and quasi-static loading assumptions. Although the adopted model was validated against centrifuge observations, three-dimensional effects, such as out-of-plane pile response, as well as additional soil constitutive features, may influence the response under actual field conditions. Therefore, the results should be interpreted as representative interaction mechanisms and comparative trends rather than complete three-dimensional field-scale predictions. Future studies should extend the present framework to three-dimensional modeling and investigate a broader range of soil conditions, foundation configurations, and faulting parameters.

CC BY

Acknowledgements

The authors would like to express their sincere appreciation to Shahid Rajaee Teacher Training University for providing the necessary facilities and support throughout this research. The authors also acknowledge the valuable guidance and constructive insights offered by colleagues at the Department of Civil Engineering. This study received no external funding.

Declaration of interest

The authors have no conflicts of interest to declare. All co-authors have reviewed and approved the final version of the manuscript, and there are no financial or personal relationships that could have influenced the work reported in this study.

Authors' contributions

Ali Safari: conceptualization, methodology, numerical modeling, data curation, visualization, writing – original draft. Ali Nabizadeh: supervision, validation, methodology, investigation, writing – review & editing.

Data availability

The datasets generated and analyzed during the current study are not publicly available but can be obtained from the corresponding author upon reasonable request.

Declaration of use of generative artificial intelligence

The authors declare that ChatGPT was used solely to assist with language editing and improving the clarity and readability of the manuscript. The artificial intelligence tool was not used for data generation, numerical modeling, analysis, interpretation of results, or formulation of conclusions. All scientific content and responsibility remain entirely with the authors.

List of symbols and abbreviations

c	Soil cohesion
h	Vertical fault offset
h/H	Normalized vertical fault offset
u_x	Horizontal displacement
u_y	Vertical displacement
z	Depth below ground surface
D	Pile diameter
E	Young's modulus (elastic modulus)
EI	Flexural rigidity of pile
E_p	Elastic modulus of pile material
FEM	Finite Element Method
H	Thickness of soil layer
I	Second moment of area of pile cross-section
L	Pile length
MPM	Material Point Method
PEEQ	Equivalent plastic strain
U	Displacement
γ	Unit weight of soil
ε	Strain
ν	Poisson's ratio
σ	Normal stress
τ	Shear stress
φ	Internal friction angle of soil
ψ	Dilatancy angle

References

Ahmed, W., & Bransby, M.F. (2009). Interaction of shallow foundations with reverse faults. *Journal of Geotechnical and Geoenvironmental Engineering*, 135(7), 914-924. https://doi.org/10.1061/(ASCE)GT.1943-5606.0000072.

Anastasopoulos, I., Antonakos, G., & Gazetas, G. (2010). Slab foundation subjected to thrust faulting in dry sand: parametric analysis and simplified design method. *Soil Dynamics and Earthquake Engineering*, 30(10), 912-924. https://doi.org/10.1016/j.soildyn.2010.04.002.

Anastasopoulos, I., Kourkoulis, R., Gazetas, G., & Tsatsis, A. (2013). Interaction of piled foundation with a rupturing normal fault. *Geotechnique*, 63(12), 1042-1059. https://doi.org/10.1680/geot.12.P.114.

Ashtiani, M., Ghalandarzadeh, A., & Towhata, I. (2016). Centrifuge modeling of shallow embedded foundations subjected to reverse fault rupture. *Canadian Geotechnical Journal*, 53(3), 505-519. https://doi.org/10.1139/cgj-2014-0444.

Baziar, M.H., Nabizadeh, A., & Jabbary, M. (2015). Numerical modeling of interaction between dip-slip fault and shallow foundation. *Bulletin of Earthquake Engineering*, 13(6), 1613-1632. https://doi.org/10.1007/s10518-014-9690-1.

Bransby, M., Davies, M.C.R., El Nahas, A., & Nagaoka, S. (2008). Centrifuge modelling of reverse fault–foundation interaction. *Bulletin of Earthquake Engineering*, 6(4), 607-628. https://doi.org/10.1007/s10518-008-9080-7.

Guan, L., Hu, C., Ling, D., & Chen, G. (2025). Experimental study on the interaction mechanisms of shallow foundations-soil under reverse fault. *Bulletin of Engineering Geology and the Environment*, 84(6), 399. https://doi.org/10.1007/s10064-025-04332-w.

Guo, D., Liu, Y., Tang, J., Zhang, Z., Yao, C., Li, Y., & Wu, W. (2025). A novel simplified analysis model to predict behaviors of single piles subjected to reverse faulting. *Buildings*, 15(3), 335. https://doi.org/10.3390/buildings15030335.

Liu, C.-Y., Li, C.-H., Chan, P.-C., Hung, C.-H., & Lin, M.-L. (2021). 3D sandbox and numerical modeling of coseismic surface rupture induced by oblique-slip faulting and its interaction with embedded shallow foundation. *Engineering Geology*, 282, 105990. https://doi.org/10.1016/j.enggeo.2021.105990.

Yao, C., & Takemura, J. (2020). Centrifuge modeling of single piles in sand subjected to dip-slip faulting. *Journal of Geotechnical and Geoenvironmental Engineering*, 146(3), 04020001. https://doi.org/10.1061/(ASCE)GT.1943-5606.0002202.

Yao, C., Takemura, J., & Zhang, J. (2021). Centrifuge modeling of single pile-shallow foundation interaction in reverse fault. *Soil Dynamics and Earthquake Engineering*, 141, 106538. https://doi.org/10.1016/j.soildyn.2020.106538.

CC BY